Modeling Three-Dimensional Groundwater Flow and Advective Contaminant Transport at a Heterogeneous Mountainous Site in Support of Remediation

Quanlin Zhou,* Jens T. Birkholzer, Iraj Javandel, and Preston D. Jordan

ABSTRACT

A calibrated groundwater flow model for a contaminated site can provide substantial information for assessing and improving hydraulic measures implemented for remediation. We developed a three-dimensional transient groundwater flow model for a contaminated mountainous site at which interim corrective measures were initiated to limit further spreading of contaminants. This flow model accounts for complex geologic units that vary considerably in thickness, slope, and hydrogeologic properties, as well as large seasonal fluctuations of the groundwater table and flow rates. Other significant factors are local recharge from leaking underground storm drains and recharge from steep uphill areas. The zonation method was employed to account for the clustering of high and low hydraulic conductivities measured in a geologic unit. A composite model was used to represent the bulk effect of thin layers of relatively high hydraulic conductivity found within bedrock of otherwise low conductivity. The inverse simulator iTOUGH2 was used to calibrate the model for the distribution of rock properties. The model was initially calibrated using data collected between 1994 and 1996. To check the validity of the model, it was subsequently applied to predicting groundwater level fluctuation and groundwater flux between 1996 and 1998. Comparison of simulated and measured data demonstrated that the model is capable of predicting the complex flow reasonably well. Advective transport was approximated using pathways of particles originating from source areas of the plumes. The advective transport approximation was in good agreement with the trend of contaminant plumes observed during the same years. The validated model was then refined to focus on a subsection of the large system. The refined model showed that most of the hydraulic measures implemented for remediation are effective.

In the late 1980s, groundwater contamination was detected at the original site (Old Town Area) of the Lawrence Berkeley National Laboratory (LBNL), Berkeley, CA (Javandel, 1990; LBNL, 2000, 2003). A detailed investigation determined the extent of contamination in soil and groundwater. Three groundwater contamination plumes were identified; each originated from a separate source, but they comingled downstream. The principal contaminants originally released at this site were perchloroethene (PCE), trichloroethene (TCE), and carbon tetrachloride. Interim corrective measures were initiated to remove or control sources of contamination and prevent further spreading of contaminants. In addition to the information on contamination, a large amount of data was also collected on geologic profiles, hydrogeologic properties, and groundwater levels in great spatial and temporal detail. Significant seasonal fluctuations in water levels were observed. The measured hydraulic conductivities demonstrate orders of magnitude variation among different hydrogeologic units and even within a given unit. The variation within a unit occurs in the form of spatial clusters of high and low hydraulic conductivities. Geologic logs sometimes show thin layers of potentially high hydraulic conductivity embedded within bedrock of otherwise low conductivity.

Flow and transport in heterogeneous porous media and fractured rocks have been investigated extensively in the last three decades (e.g., de Marsily, 1986; Dagan, 1989; Gelhar, 1993; Bear et al., 1993; Rubin, 2003). Three different methods can be employed to represent the spatial distributions of hydrogeologic parameters (e.g., hydraulic conductivity), depending on the available data on hydrogeologic parameters and system responses (e.g., water level and flux), and investigation objectives. The first method often assumes that a hydrogeologic parameter distribution may be represented as a stationary or nonstationary random field in space with known statistical properties. A stochastic analysis based on perturbation analysis or Monte Carlo simulation is often used to investigate the large-scale system responses as influenced by the smaller-scale heterogeneity (Gelhar and Axness, 1983; Tompson and Gelhar, 1990; Tsang et al., 1991). This stochastic method can provide a general picture of flow and transport in the heterogeneous subsurface using statistical moments. However, it may not be applicable for characterizing a contaminated site requiring remediation, where detailed deterministic description of local flow and transport features is critical to the efficiency of restoration measures. In the second method, the spatial variability of a hydrogeologic parameter is deterministically characterized using all available data on measurements of this parameter and measured system primary variables. Often, the parameter in question is estimated from calibration of the model against known system responses, such as against groundwater level data in wells (Sun, 1994; Finsterle, 1999; Bandurraga and Bodvarsson, 1999; Castro and Goblet, 2003). The spatial variability at a smaller scale is usually neglected, and its effects on flow and transport are assumed to be incorporated in the estimated properties (Bodvarsson et al., 2001). This practical method can improve prediction accuracy because the information on measured system responses is already incorporated into the developed model. The method is applicable when data on both hydrogeologic parameters and system responses are sufficient, which is often the case for many site characterization studies (e.g., Bodvarsson et al., 1999; Smith

Q. Zhou, J.T. Birkholzer, I. Javandel, and P.D. Jordan, Earth Sciences Division, Lawrence Berkeley National Laboratory, University of California, Berkeley, CA 94720. Received 8 Oct. 2003. Special Section: Research Advances in Vadose Zone Hydrology through Simulations with the TOUGH Codes. *Corresponding author (qlzhou@lbl.gov).

Published in Vadose Zone Journal 3:884–900 (2004).

677 S. Segoe Rd., Madison, WI 53711 USA

Abbreviations: LBNL, Lawrence Berkeley National Laboratory; PCE, perchloroethene; TCE, trichloroethene; VOC, volatile organic compound.

et al., 1997). The third method combines stochastic and deterministic approaches. It assumes that the distribution of a hydrogeologic parameter can be represented by a layer-scale mean superimposed by stationary perturbations in a multilayered medium (e.g., Zhou et al., 2003).

In this study, a three-dimensional groundwater flow model is developed using the simulator TOUGH2 to assess the performance of corrective measures implemented at the contaminated Old Town site. Although the present study deals specifically with the saturated zone, TOUGH2 is a multiphase code applicable to vadose and saturated zone contaminant flow and transport. The deterministic method described above is used to calibrate the model. A large amount of measurement data on hydraulic conductivity, groundwater level, and water flux is used for this task. A composite single continuum approach is employed, with the aid of "effective" porosity, to represent the bulk effect of thin layers of relatively high hydraulic conductivity embedded within bedrock of otherwise low conductivity. We first briefly describe the groundwater contamination plumes and interim corrective measures at the LBNL Old Town site. Next, the groundwater flow model is developed, starting with the hydrogeologic framework model. The model boundary and boundary conditions are determined using the groundwater level measured at a large number of monitoring wells. Rock properties in a number of rock zones and the infiltration rate in leaking storm drains are adjusted to calibrate the model for observed responses. The calibrated model is then validated using a blind prediction against measured groundwater level series and flow rates. Advective transport patterns, represented using pathways of particles originating from source areas of plumes, are also employed for the validation. Finally, on the basis of the calibrated and validated site-scale model, a refined flow model is developed for the central area of the main plume. The efficiency of the interim corrective measures implemented for restoration is assessed from analysis of advective pathways.

Old Town Site Description

The Old Town site is located within the Lawrence Berkeley National Laboratory, Berkeley, CA (Fig. 1). Lawrence Berkeley National Laboratory is located on the Oakland-Berkeley Hills, with surface elevations ranging from approximately 150 to 305 m above mean sea level. The center of the Old Town area is located in a relatively flat part of the mountainous site. This central part is surrounded by a steep uphill slope to the northeast and by steep downhill slopes to the west and south.

A considerable amount of data on geologic profiles and hydrogeologic properties has been collected. The top geologic units (of interest to the investigation of groundwater flow and contaminant transport) are, starting from the ground surface, surficial soils (including artificial fill and alluvial–colluvial deposits), Moraga unit, Mixed unit, and Orinda unit. The hydrogeologic complexity of the mountainous and urbanized site is composed of three major aspects: (i) accentuated morphology, with steep hills, deep ravines, and large gradients; (ii) complicated geologic structure, with several units of vastly different hydrologic properties; and (iii) local infiltration, from known and unknown leakage of underground storm drains and other facilities. For the detailed geology, readers are referred to LBNL (2000).

During the last decade, approximately 100 monitoring wells have been installed to measure water levels and hydraulic conductivities in the subsurface and to characterize and monitor the distribution of contaminants in the groundwater at the site. The primary contaminants detected in the groundwater in the Old Town area are halogenated nonaromatic volatile organic compounds (VOCs) and fuel hydrocarbons (LBNL, 2000, 2003). The VOCs are the most widespread contaminants and are present in a broad multilobed plume that covers the central part of the area. The contaminants are characterized primarily from groundwater samples collected from monitoring wells. Based on both the distribution of individual chemicals and the constituent and aggregate concentrations, three apparently distinct plume lobes (B7, B52, and B25) can be distinguished (Fig. 2). The vertical distribution of contaminants shows that contaminants exist in the upper portion of the saturated zone; significantly lower or no concentrations have been detected in deeper wells. A steep concentration gradient exists across the contact between the Moraga and Orinda units in most of the plume area.

The highest concentration of contaminants in the groundwater was detected in the B7 lobe, which originates from an abandoned sump northwest of Building 7 (Fig. 2). For lower concentration lines (<100 $\mu g\ L^{-1}$), two trends are distinct. The south portion of the core plume migrates northwest to Building 58, while the north edge of the core plume tends to move northward to Building 46. The primary source of contaminated groundwater was leakage and overflow from the sump. Concentrations are as high as 300 000 $\mu g\ L^{-1}$ in the groundwater just downgradient of the abandoned sump. In the discussion that follows, the main focus is on the B7 plume, as the concentrations in the other plumes are well below those detected in the B7 lobe.

To contain and eventually clean the B7 contamination four interim corrective measures consisting of extraction and treatment of groundwater were implemented (Fig. 2). The B7 collection trench was installed immediately downgradient from the source of the B7 lobe as a source control measure. Groundwater was pumped from extraction wells in the gravel-filled trench, treated by a granular activated C system, and reinjected into the gravel-filled excavation at the former sump location. The B53-58 slope collection trench was installed in late 1998, as a source control measure in the downgradient portion of the B7 lobe core area and as a way to prevent further migration of contaminated groundwater. Continued groundwater extraction was expected to capture the core of the plume lobe between Buildings 7 and 58. The third groundwater collection trench, the B58 trench, was installed west of Building 58 in 1998 to control further migration of the B7 lobe to its downgradient extent. The fourth measure, the B46 subdrain, was in-

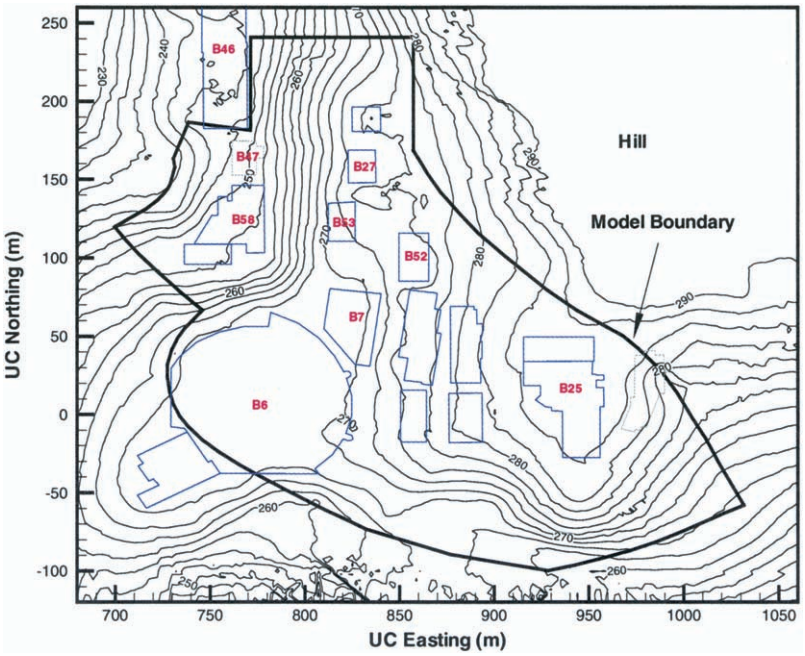

Fig. 1. Location of the Lawrence Berkeley National Laboratory Old Town site, representative buildings (blue polygons) with building numbers, and contours of the ground-surface elevation (m above mean sea level) (black solid lines).

stalled as part of a landslide mitigation measure. It collects subsurface water draining from the hillside to the east, which is subsequently treated and reinjected.

DEVELOPMENT OF GROUNDWATER FLOW MODEL

Based on the geologic data and the monitored flow and transport features at the Old Town site, a three-dimensional groundwater flow model was developed. The major modeling challenges were (i) developing a consistent hydrogeologic model honoring the complexity of the stratigraphy, (ii) determining the extent of the model domain and defining appropriate boundary conditions at the mountainous site, (iii) accurately estimating infiltration by rainfall through unpaved areas in the urbanized site and infiltration through leaking storm drains, and (iv) calibrating the model to represent the strongly heterogeneous rock properties.

Geologic Model

A geologic model is developed for the site, based on geologic data available from a total of 711 boreholes and wells, an outcrop map, a geologic map, and cross sections. From these data, the location of structural surfaces and the thickness of the hydrogeologic units are interpolated throughout the site using a Kriging algorithm (Isaaks and Srivastava, 1989; Deutsch and Journel, 1998). Contacts from the geologic map based on boring and outcrop data are used as zero-thickness data points to better constrain the lateral extent of the hydrogeologic units. The geologic model consists of the top four geologic units that contribute to groundwater flow. The top elevations of the four units are obtained on a fine horizontal two-dimensional grid and subsequently used for the three-dimensional mesh generation. Note that numerically we have four elevation surfaces (for the top of each unit), which are continuous in the study domain, even though we may have isolated masses of a unit. When a unit is absent, the top elevation of this unit is identical to the top elevation of the underlying unit, which is present.

The Moraga unit is the most permeable and therefore most important unit for groundwater flow and transport at the Old Town site. The most prominent feature about this unit is that it does not form a continuous stratigraphic unit in the model area, but rather exists in three major, isolated masses. Each of these masses has considerable thickness with maximum values between 10 and 26 m, while the top elevation of the underlying unit (the Orinda and Mixed unit) forms a deep valley or "bowl." Figure 3 shows the thickness of the Moraga unit and the top elevation of underlying unit, as given by the geologic model, and demonstrates the unique setting of the three isolated masses. The first one, referred to as Large Bowl, is located in the area of Buildings 27, 52, and 53 in the north (see also Fig. 4 for cross sections). The maximum thickness is about 26 m, and groundwater flows in the highly permeable zone from the northeastern upstream boundary downward to Building 46. The second Moraga bowl, referred to as Small Bowl, partially underlies Building 6, with a maximum thickness of about 10 m. This bowl is smaller, but potentially important because contaminants may spread within this bowl, then flow toward Building 58 to the west and potentially migrate further downhill to urban areas (Fig. 2). In the south, the so-called South Bowl underlies Building 25.

Underlying the Moraga unit is the Orinda unit, which is present in the entire model area. On average, the Orinda unit is much less permeable than the Moraga unit, and almost acts as an aquitard for the overlying Moraga unit. Nevertheless, the Orinda is an important unit for the groundwater flow and transport, as it is the only continuous water-bearing unit connecting the isolated Moraga bowls. In some areas, the Mixed unit

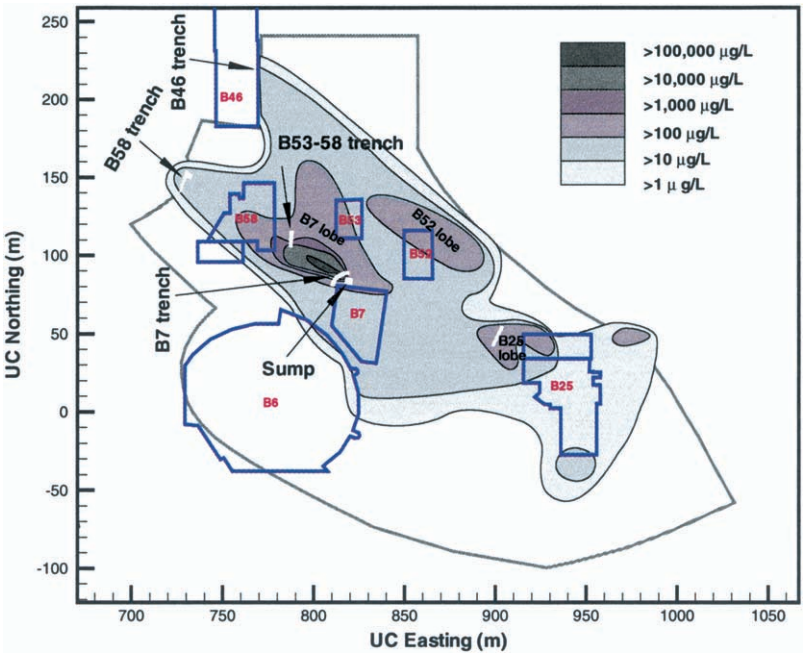

Fig. 2. Contaminant plumes observed at the Lawrence Berkeley National Laboratory's Old Town site in 2003 (gray flood) and groundwater collection trenches (white polygons) installed for restoration.

was identified at the contact between the Moraga and the Orinda. The Mixed unit, also having a low permeability on average, is mainly present in the area of the main contaminant plume, with a maximum thickness of about 9 m. Note that surficial soils are not important for groundwater flow and transport in the Old Town area because the groundwater level mainly fluctuates within underlying units. Certain parts of the site have been artificially filled to create a flat ground surface.

The unique hydrogeologic setting with three perme-

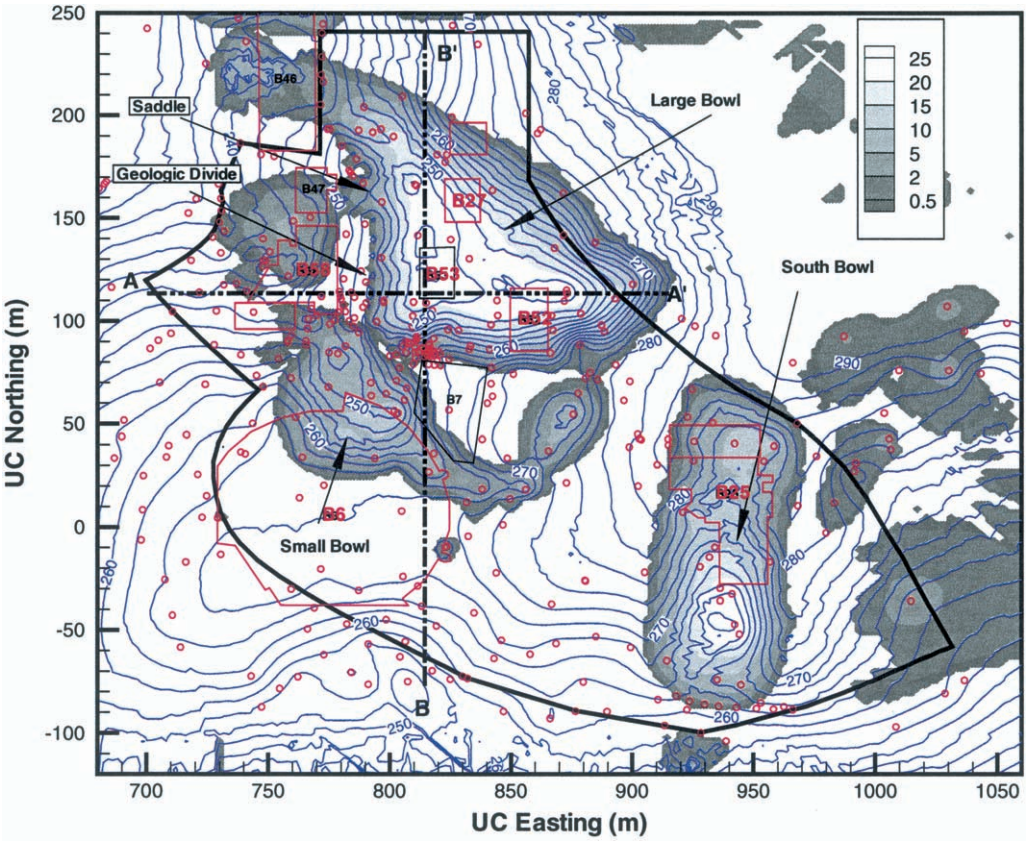

Fig. 3. Thickness contours of the Moraga unit (in gray-scale flood)) and the top elevation contours (blue solid lines) of the underlying Orinda unit (or Mixed unit, if present). Also shown is the location of all boreholes and wells (circles) used to determine the geologic model, as well as the model boundary (thick solid line). Note the location of the geologic divide and the saddle.

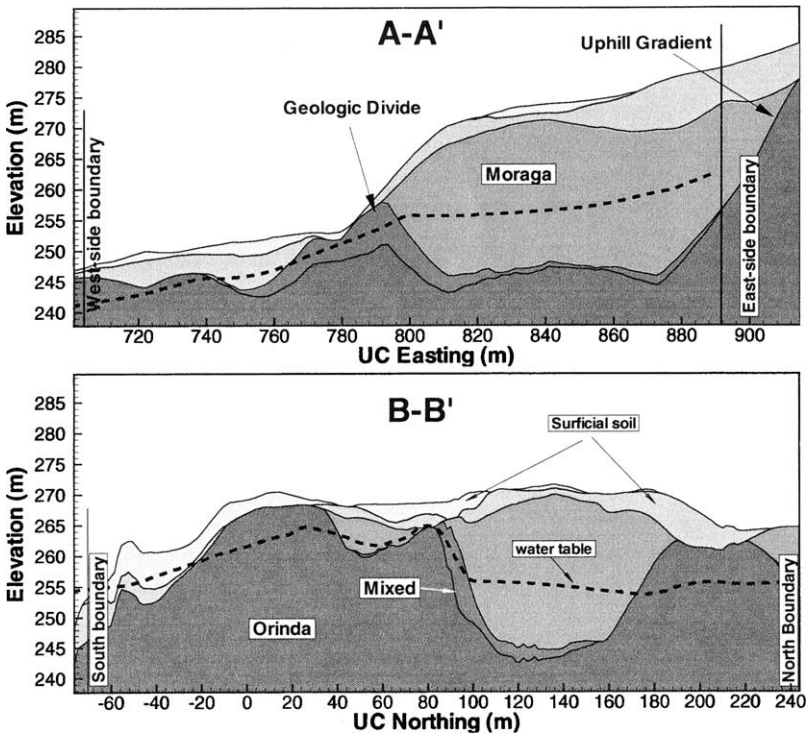

Fig. 4. Geologic profiles along the east–west axis (A–A′) and the south–north axis (B–B′), obtained in the geologic model and the representative average groundwater level along the two cross sections (dashed lines).

able bowl-shaped rock masses embedded in less permeable bedrock is an important factor for determining the transient groundwater system at the Old Town site. Groundwater may fill these permeable bowls during the wet seasons, and a significant amount of water can leave these bowls only if a given water level is reached where outflow is possible. Figures 3 and 4 also show that steep gradients of the bottom surface of the Moraga unit exist along the edges of these bowls, particularly in Large Bowl. For example, along the northern edge of Building 7, the large gradient of this unit makes it difficult to maintain a high groundwater level in the core area of the Building 7 plume. However, this high groundwater level was observed in a number of monitoring wells.

Figures 3 and 4 indicate that a geologic divide exists between Large Bowl and the area downstream of Building 58. This divide is formed by the low-permeability Mixed and Orinda units, potentially blocking westward groundwater flow from the isolated rock mass of Large Bowl. On the east of the divide is the thick, water-bearing Moraga unit. On the west is a steep downhill slope of the ground surface. This divide prevents groundwater flow in the east–west direction and forms the constrained channel for groundwater flow in Large Bowl. The divide may explain the coexistence of two separate trends of the contaminant plume originating along the north edge of Building 7. As shown in Fig. 2, the main plume forms within the Mixed unit toward Building 58, while a smaller plume exists in Large Bowl toward Building 46. Note also that a saddle at the lower top elevation of the Mixed or Orinda unit exists within this divide on the east of Building 47. This saddle is overlain by a thin layer of the Moraga unit. It may provide a pathway for groundwater flow through Large Bowl to the west when the groundwater level is high enough (e.g., in winter seasons).

Model Domain and Boundary Conditions

As described above, interfaces between different geologic units vary significantly in elevations, resulting in strong spatial changes in local groundwater characteristics, such as the groundwater level and flux. The groundwater system also shows strong fluctuations in the groundwater level and flow rate under the influence of seasonal rainfall patterns. As a result, determining model domain and conditions on the model boundary is critical to the simulation of groundwater flow and contaminant plumes.

As shown in Fig. 2 and 3, the model domain includes the three major contaminant plume lobes (B7, B52, and B25) and all three water-bearing Moraga bowls (Large, Small, and South Bowl). Outside of the model domain, few wells are available for evaluating geologic logs and measuring the water level, and thus the hydrogeologic model is not as accurate as within the model domain. The model boundaries are placed along monitoring wells, so the measured water-level values can be used as boundary conditions. As shown in Fig. 5, the boundary follows eight monitoring wells (e.g., MW46-93-12 and MW52-94-10). In some locations, where monitoring wells are not available, no-flow boundaries are defined based on information on flow paths determined from the water-level data. At some critical locations along the boundary, monitoring wells away from the boundary are projected out to the model boundary. For example, Well

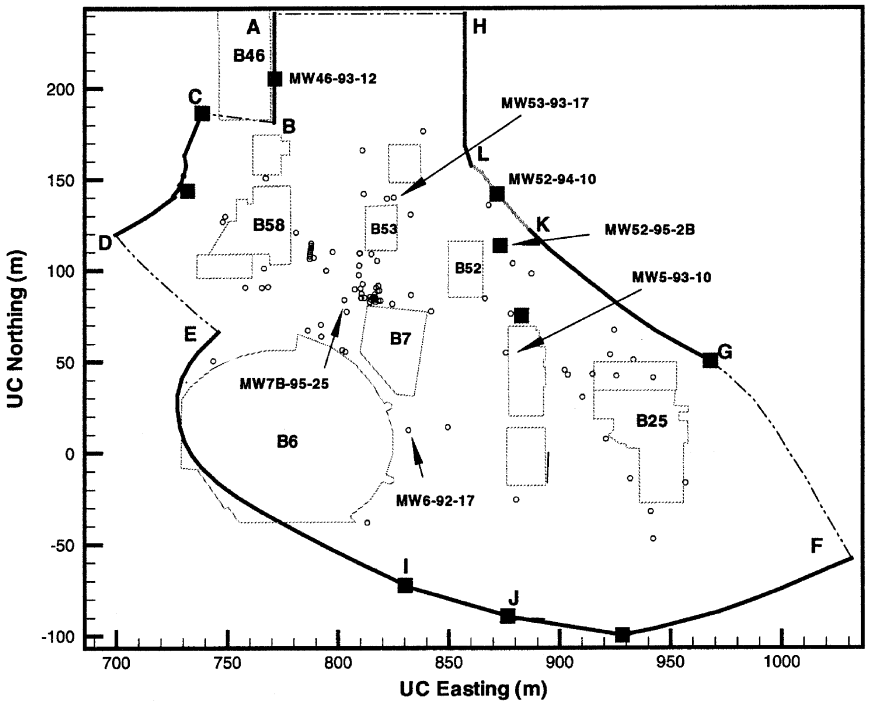

Fig. 5. Model boundary with four different boundary segment groups (thick solid lines) (A–B, B46 group; C–D, B58 group; E–F, B6-Lawrence-Road group; and G–H, upstream group) and four no-flow boundary segments (dotted-dashed lines). Also shown are monitoring wells in the model domain (circles) and on the boundary (filled squares).

MW52-95-2B is projected to the boundary to better constrain the significant water flux entering the model domain from the upstream hillside through the Moraga unit. For the calibration and validation of the groundwater flow model, the measured groundwater levels at the boundary wells are used as boundary conditions. For future prediction with unknown groundwater level in the boundary wells, the average annual groundwater level may be used because the seasonal pattern of groundwater level changes is fairly consistent across years.

The model boundary consists of four boundary segment groups with prescribed groundwater levels and four no-flow boundary segments connecting these groups (Fig. 5). Each of the segment groups consists of at least one boundary segment, with either uniform or linearly varying groundwater level. All these first-type conditions are time dependent, with varying magnitudes of seasonal changes. Of the upstream segments under the first-type condition, Segment KL along Large Bowl is most important because the major fraction of the boundary inflow is through this segment, referred to as the "B52 influx" segment. This segment represents the significant amount of groundwater flowing from the uphill region down into the model domain. Of all the downstream boundary segments, the B46 segment, located at the eastern edge of Building 46, is most important to groundwater outflow. A groundwater collection trench, the B46 trench, extends along this boundary segment where contaminated water was collected for remediation. The B58 boundary segment located near Building 58 and the B58 trench accounts for a smaller fraction of the total outflow.

Recharge and Leakage of Storm Drains

Groundwater flow at the site is strongly affected by direct infiltration from rainfall, as well as from leakage out of storm drains and other underground utilities. Careful estimate of infiltration from these water recharge sources is essential for the model, because the seasonal fluctuations of the groundwater level are strong in most of the system, indicating that recharge is an important contribution to water balance.

The areal net recharge through the unpaved areas of the model area is calculated from the rainfall intensity, the size of the unpaved areas, and a recharge factor (fraction of rainfall infiltrating into groundwater). Appropriate recharge factors are estimated from the slope of the topography and the properties of the surficial soil. Some buildings also contribute to direct infiltration because the rainfall on their roofs directly drains into neighboring soil areas. In all paved areas, like parking lots or streets, a small recharge factor of 0.02 is used to represent unaccounted infiltration through small flower beds and pavement joints and cracks, which are too small to be included individually. Figure 6a shows the four types of infiltration areas defined based on the types of land surface coverage and slope of topography. In each type of infiltration area, further classification is conducted based on the properties of the surficial soil.

Evidence of corroded metal pipes and ruptured concrete pipes was observed in the field (Fig. 6b). While leakage through such storm drains is critical to the local groundwater system, estimating the amount of leaking water is difficult because it depends on many parameters, such as catchment area, type of damage, and soil

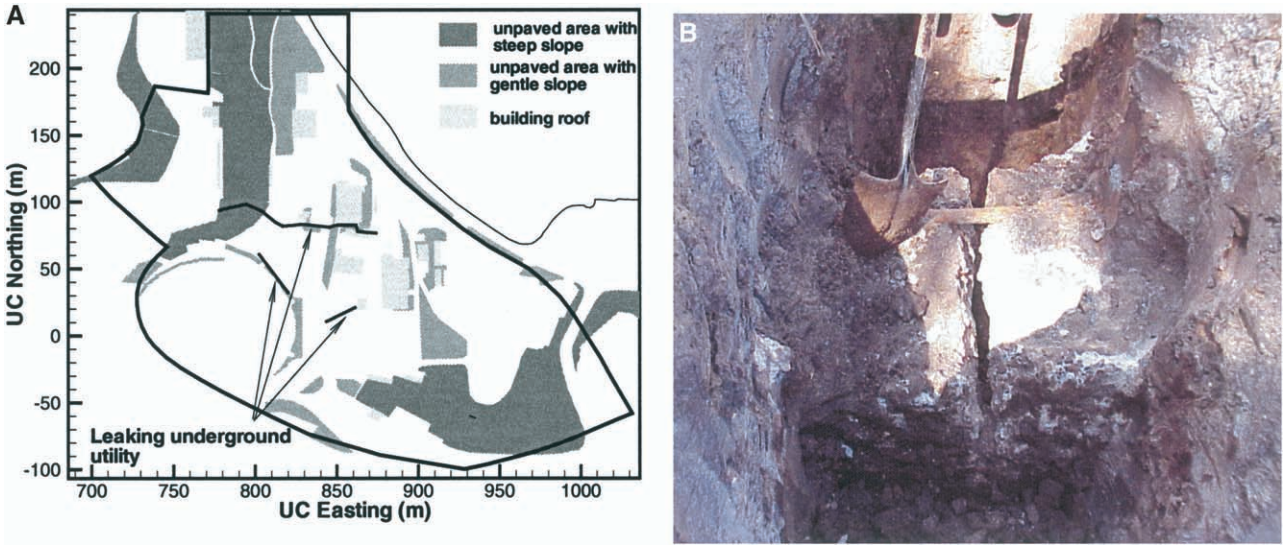

Fig. 6. (A) Three different types of infiltration areas in addition to the default paved area, and three detected leaking storm drains and other underground utilities. (B) Evidence of ruptured concrete pipes observed in the field.

type. In the model, storm drain leakage is calibrated in a systematic manner. First, subsurface utility maps are employed to locate potential leakage from corroded storm drains. Second, for each of the corroded storm drains, the number of pipe segments contributing to leakage and their corresponding discharge catchments are determined. Third, a simple pipe model is developed based on water balance without considering changes in mass storage inside a pipe segment. Finally, the recharge factor for each segment is calibrated (with rock properties) using the measured groundwater level at monitoring wells.

In the Old Town area, three locations are confirmed to have a significant amount of water leaking out of storm drains or other underground utilities. These locations are schematically depicted in Fig. 6a. The storm drain located in the northern edge of Building 7 consists of four pipe segments with different catchment areas. Different recharge factors are obtained through calibration for these four segments.

Heterogeneity Calibration

Hydraulic conductivity measurements and geologic logs obtained at the site indicate strongly heterogeneous conditions. The first type of heterogeneity at the site is the spatial variability of hydraulic conductivity among different hydrogeologic units. The second is the spatial variability of hydraulic conductivity within a geologic unit, with clusters of low and high values. This variability results from lateral depositional differences parallel to bedding. For the Moraga unit, hydraulic conductivities vary across individual landslide blocks, with higher conductivities typically near the center of a block and lower conductivity near the edge. For the Mixed and Orinda unit, hydraulic conductivities vary due to varying proportions of more or less permeable lithologies. For instance, the higher proportion of medium to coarse-grained sandstones and pebbly sandstones, within the Orinda unit to the north and northwest of Building 25, causes a higher bulk conductivity in this area than was measured in the Orinda unit elsewhere. The final type is the structural heterogeneity resulting from depositional differences perpendicular to bedding, especially the interlayering of different lithologies, within each unit. This is most prominent in the Mixed and Orinda units, but it also occurs within the Moraga unit to some extent. Capturing the three different kinds of heterogeneity in the model is critical to the accurate prediction of groundwater flow and contaminant transport.

The first two types of variations in hydraulic conductivity discussed above are exhibited in the measured hydraulic conductivities. About 100 measurements were obtained in the Old Town area using slug tests, pumping tests, and tracer tests. Most of the measurements in the model domain were conducted while screening in the Moraga and Orinda units. While permeability values in the surficial soils have also been measured and calibrated, in our below discussion we focus on the three water-bearing units, the Moraga, the Mixed, and the Orinda unit. The geometric means of hydraulic conductivity for these units are 2.81×10^{-6}, 9.50×10^{-8}, and 4.27×10^{-8} m s^{-1}, respectively. The respective standard deviations of log hydraulic conductivity are 1.35, 1.25, and 1.42. These large standard deviations indicate considerable heterogeneity. For example, the measured hydraulic conductivities of the Moraga unit vary within five orders of magnitude at the site. The most permeable Moraga zone is located in Large Bowl, with a maximum value of 3.98×10^{-4} m s^{-1}, whereas the smallest Moraga conductivity is located in the north edge of Building 7, with a value of 1.26×10^{-9} m s^{-1} (Fig. 7). In addition to the strong spatial variability, the measured hydraulic conductivities demonstrate another important characteristic: different clusters of distinct hydraulic conductivity values in different areas. For example, the eight measured hydraulic conductivities at different locations within Small Bowl are very consistent, producing a standard deviation (of log hydraulic conductivity) of 0.32.

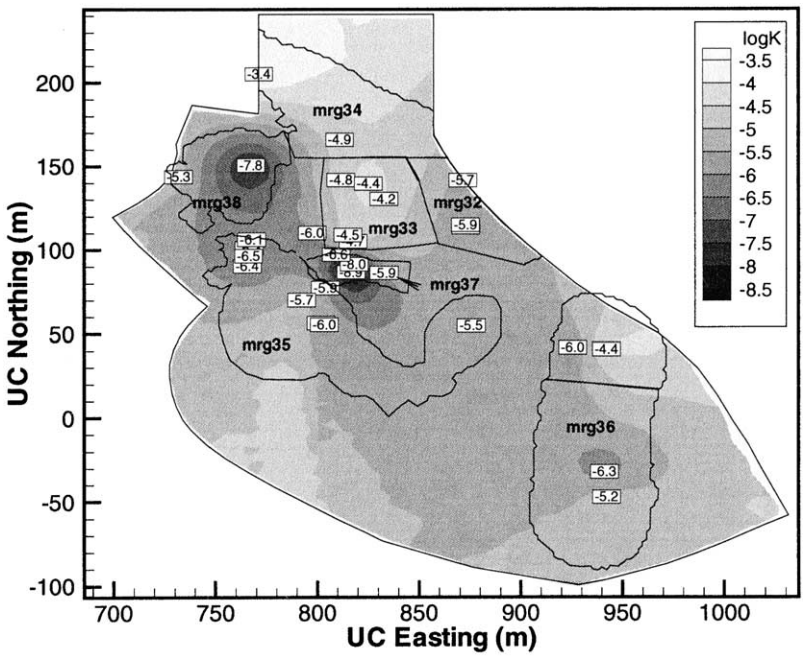

Fig. 7. Contour of the log measured hydraulic conductivity in the Moraga unit with the original measured values, and eight rock zones defined.

This clustering can be seen in Fig. 7 from the contour of log measured hydraulic conductivities in the Moraga unit. Such clusters are unique to this geologic setting where isolated rock masses were deposited in various landslide events (LBNL, 2000).

The different hydrogeologic units are modeled as separate rock units by incorporating the geologic model in the computational mesh. Within each unit, various rock zones are defined to account for the lateral variability of rock properties, with spatially homogeneous rock properties assumed within each zone. The rock zone method is appropriate to the site modeling for two reasons. First, local groundwater flow features—and thus deterministic characterization of heterogeneity—are critical to contaminant remediation at the site. Second, rock properties in each rock zone can be accurately calibrated by making full use of information from both measured rock properties and groundwater level data at numerous monitoring wells. The rock zones are defined based on the clustering characteristics of measured hydraulic conductivities, the discontinuity of rock masses, and the availability of monitoring wells. There are eight, five, and four rock zones for the Moraga, Mixed, and Orinda units, respectively.

Four different kinds of information indicate the presence of the third type of heterogeneity, which is that thin layers of relatively high hydraulic conductivity exist within bedrock of otherwise low conductivity at the site, particularly in the Mixed and Orinda units (Fig. 8). First, geologic logs frequently indicate that thin permeable sandstone layers are present within siltstone layers. Second, water level responses in multilevel wells, screened in the Orinda unit at the scale of individual beds, indicate significant hydraulic differences between the beds. Third, many wells allow pumping only for a limited time, indicating that the water storage in the vicinity of these pumping wells is small. Finally, the net infiltration caused by rainfall is insufficient to cause the observed seasonal water-level fluctuations if the measured porosities are used throughout a hydrogeologic unit. While only comprising a small fraction of the Mixed–Orinda

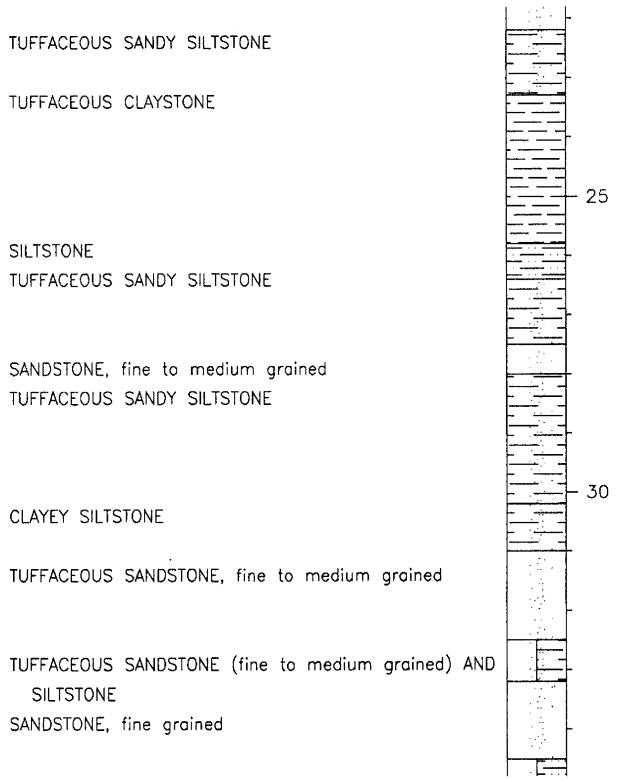

Fig. 8. A sample geologic log showing thin layers of high hydraulic conductivity, fine- to medium-grained sandstone layer at depth of 8.5 m (28 feet) from the ground surface, within bedrock of low hydraulic conductivity.

rock, the thin conductive sandstone layers may provide fast flow paths important for transport.

Because the occurrence of the sandstone layers cannot be sufficiently mapped, a single continuum approach is used in the groundwater flow model. A composite model is applied to represent the bulk effect of the composite medium comprising thin layers of large hydraulic conductivity within almost impervious rock. In this model, comparable small porosity values are defined as representing the "effective" porosity of the composite medium, causing a large and fast groundwater level response to rainfall events.

The iTOUGH2 code (Finsterle, 1999) is used to calibrate the hydraulic conductivity and the "effective" porosity value in each of the defined 17 rock zones within the geologic units. In a first step, the geometric mean and standard deviation of hydraulic conductivity in each rock zone are calculated using the available measurements. The former is used as the prior value, while the latter is used to weight the difference between the calibrated and the prior values in the objective function. The objective function also includes the misfit between the measured and calibrated transient water level processes in a number of monitoring wells, and the misfit between calibrated and collected flow rate in the groundwater collection trenches at Buildings 46 and 58. The calibration process is to reduce the objective function by adjusting calibration parameters and to improve the match between calibrated and measured values. A transient calibration is conducted, using data collected between 1 July 1994 and 30 June 1996.

To obtain realistic and accurate rock properties using the transient measured groundwater level and flow rate, four separate but interconnected groundwater subsystems are defined based on their flow characteristics. The calibration is conducted in two steps. In the first, rock properties specific to a subsystem are calibrated independently, using the measurements within the subsystem. In the second, rock properties for more than one subsystem are calibrated using all measurements in the entire groundwater system. This calibration method is used to avoid unphysical results obtained using the do-it-all-at-once method, which produces very small seasonal fluctuations around the mean groundwater level at some monitoring wells. This calibration process leads to a good match between the measured and the calibrated transient-water-level processes in most monitoring wells, as further discussed below in Model Validation.

Figure 9 shows the calibrated hydraulic conductivity in each of the 17 rock zones for the Moraga, Mixed, and Orinda units, together with the measured hydraulic conductivities and their geometric mean (used as prior information in calibration). The calibrated hydraulic conductivity in the eight rock zones of the Moraga unit varies over three orders of magnitude. For rock zone mrg37, located in the north edge of Building 7, the Moraga unit is least permeable in comparison with all other Moraga rock zones. The most permeable Moraga rock zone is mrg34, located in the downstream end of Large Bowl. The calibrated hydraulic conductivity in the five rock zones of the Mixed unit varies by less than one order of magnitude. In the Orinda unit, the calibrated hydraulic conductivities in four rock zones are close to each other except in the ord52 zone, which is located in the vicinity of the upstream boundary and the northern area of Building 25. The calibrated high value is consistent with the four measured hydraulic conductivities of the Orinda unit in this area.

Note that the differences obtained between the calibrated and measured hydraulic conductivities of a rock zone depend on the quality of the measurements. The calibrated and the measured hydraulic conductivities are typically close to each other when the measurements have been conducted with pumping tests (e.g., in the Moraga unit). Large differences occur between the calibrated and the measured hydraulic conductivities in the Mixed unit. Here, the number of available measurements is small, and the data were obtained using slug tests, which are less accurate than those obtained by pumping tests.

The calibrated "effective" porosities are smaller than the actual physical porosities in all rock zones. Typical

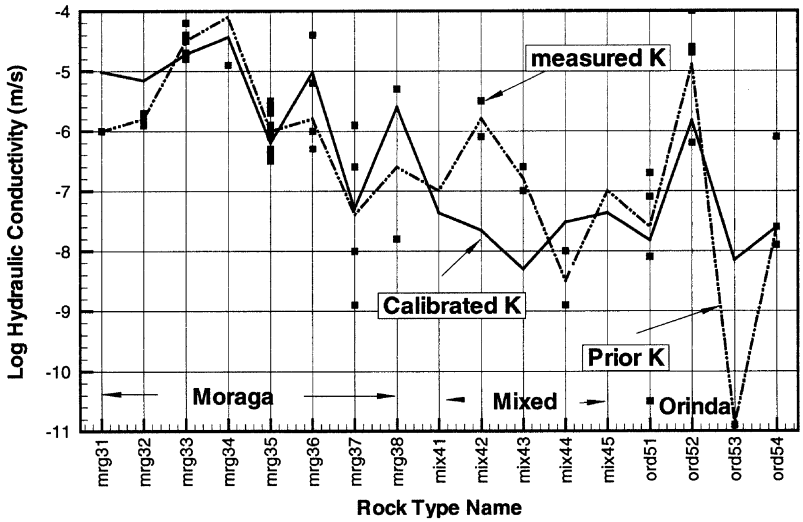

Fig. 9. Calibrated hydraulic conductivity vs. its prior value, and measured hydraulic conductivities for each of the 17 defined rock zones.

total porosities, as estimated from sample analysis, are 0.29 for the Moraga unit, 0.35 for the Mixed unit, and 0.25 for the Orinda unit. In contrast, the calibrated "effective" porosities are much smaller, at about 0.05, 0.02, and 0.03 for the three units, respectively. Such small porosities result in a fast response of the groundwater level to infiltration events, which is consistent with the significant fluctuations observed in monitoring wells during both wet and dry seasons. The small "effective" porosity is also consistent with field observations that pumping was not possible for long time in wells with significant fluctuations in the groundwater level. As a percentage of the total porosity, the "effective" porosity is typically 17% in the Moraga unit, 6% in the Mixed unit, and 12% in the Orinda unit. This accords well with rock core observations from each unit, which indicate that the Moraga unit typically contains the highest percentage of relatively more conductive layers, and the Mixed unit typically contains the lowest percentage of relatively more conductive layers.

MODEL VALIDATION

The calibrated flow model is validated by conducting a blind prediction for the period between 1 July 1996 and 30 June 1998. This validation is based on the comparisons between (i) measured and predicted water levels at a large number of monitoring wells, (ii) collected and predicted flow rates at the B46 trench located at the model boundary, and (iii) the measured trends of contaminant plumes and the predicted advective transport based on particle pathways.

Groundwater Flow Results

In this section, we first present and discuss the transient groundwater flow patterns for two representative time snapshots during a typical dry summer season and a typical wet winter season. Analysis of the goodness of fit between the calibrated model and the measured water-level data is conducted in a second step.

Figure 10 shows the groundwater level contours and flow velocity fields predicted for August 1997 (representing dry, summer seasons) and for March 1998 (representing wet, winter seasons). Four distinct groundwater subsystems are classified for ease of interpretation and explanation of the global groundwater flow features (Fig. 10). The first subsystem, Large Bowl subsystem, represents groundwater in the area of the Large Bowl, where the hydraulic conductivity is relatively high. The second one is referred to as the Small Bowl subsystem located in the area of Small Bowl. The third one is referred to as the B7 subsystem, located between Large and Small Bowls and underlying Building 7. The core of the main B7 plume is located in this subsystem, where the groundwater level is relatively high and the hydraulic conductivity is relatively small compared with neighboring units. Finally, the South Orinda subsystem is located in the south area, with groundwater flowing primarily within the Orinda unit.

In the Large Bowl subsystem, the groundwater flow rate is much larger than that in the other three subsystems in both dry and wet seasons. Groundwater flows within the thick Moraga bowl from the upstream boundary southeast of Large Bowl to the downstream boundary located at Building 46 (Fig. 5). Water flows via a channel of the saturated Moraga unit from the upstream boundary to the downstream one. The water-bearing cross-sectional area of the channel varies from the southeast to the northwest. The smallest area of the Building 46 boundary leads to the maximum velocity in the subsystem. In wet seasons, the recharge to the Large Bowl subsystem is from inflow through the upstream boundary, from infiltration by rainfall and through the leaking storm drain located at the northern edge of Building 7, and from discharge from the South Orinda subsystem caused by steep hydraulic gradients. In dry, summer seasons, groundwater flow results from the inflow through the

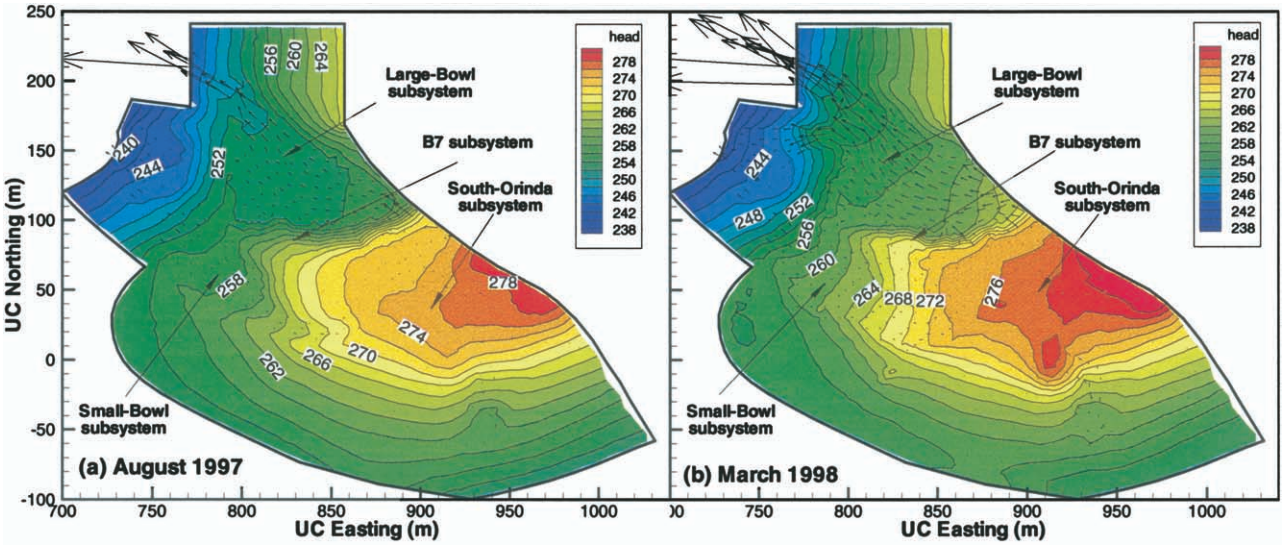

Fig. 10. Simulated groundwater level contours and flow velocity fields on the water table in (a) August 1997 (dry season) and (b) March 1998 (wet season).

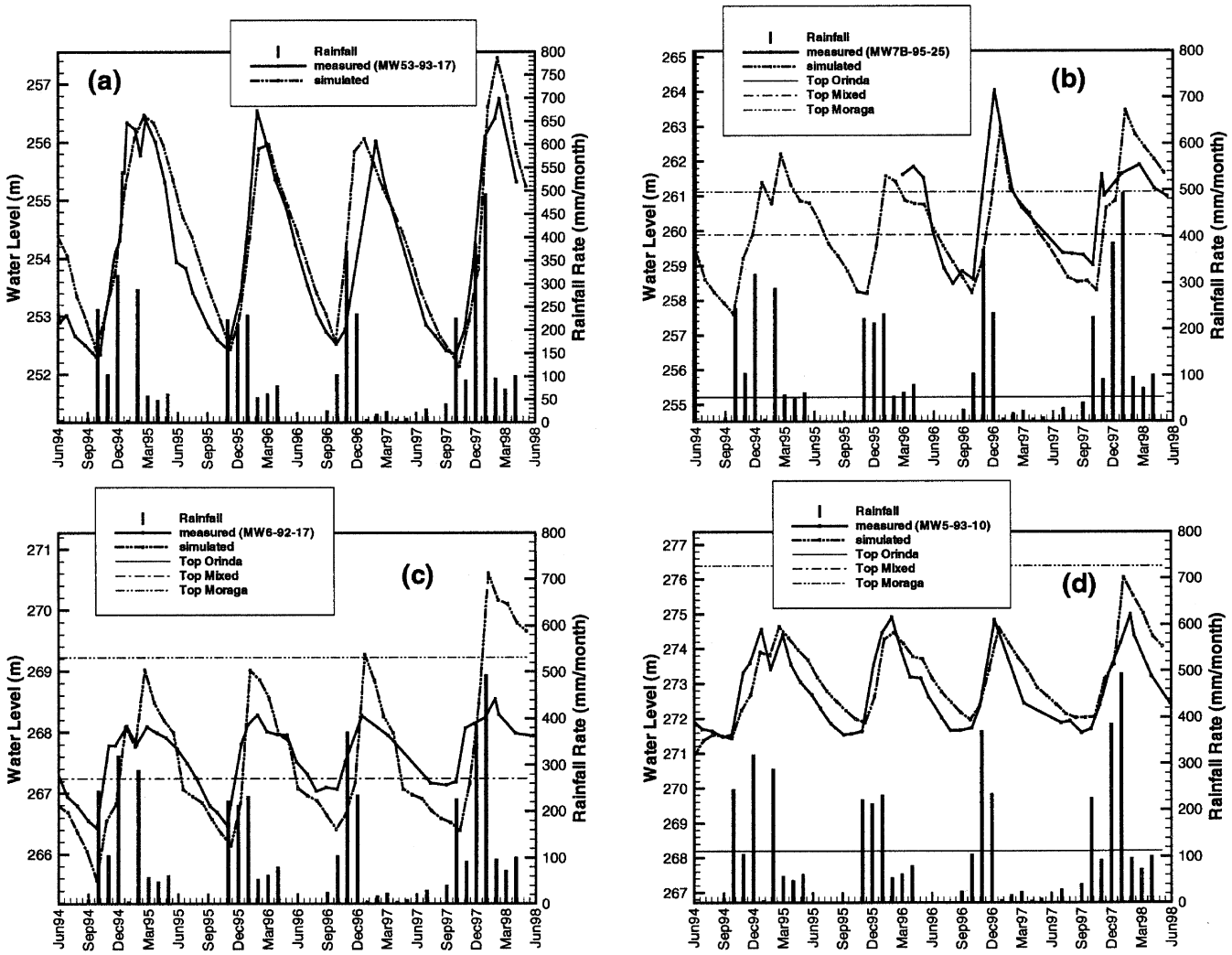

Fig. 11. Comparison of the measured and predicted water level at a representative well in each of the four groundwater subsystems with the top of each hydrogeologic unit shown by horizontal lines.

upstream boundary and from the South Orinda subsystem. From dry seasons to wet seasons, the groundwater level rises significantly, causing increases in the total flow-bearing cross-sectional area of the channel and the overall flow rate in the bowl.

The transient fluctuations in the groundwater level can be clearly seen from the groundwater level histogram at MW53-93-17, a representative monitoring well located in the center of Large Bowl. Figure 11 shows both the measured and the simulated groundwater level in this well (Fig. 11a) and in three more wells representative of the other subsystems (Fig. 11b–11d), using data collected between 1994 and 1998. This time period comprises the calibration period (1994–1996) and the validation period (1996–1998), and thus provides information on the accuracy of the model, as discussed more below. The response of the groundwater level at Monitoring Well MW53-93-17 to recharge from infiltration and from the upstream boundary is fast. The time scale for the groundwater level to rise from the lowest to the highest value is usually <1 mo. The overall amplitude of the groundwater level changes is approximately 4.3 m (14 feet).

As already mentioned, a geologic divide extends from the south to the north along the west edge of the Large Bowl with a saddle of lower top elevation roughly in the middle. As shown in Fig. 10a, groundwater in Large Bowl cannot flow westward through the divide in dry seasons because the groundwater level does not reach the top elevation of the divide. In wet seasons, however, the groundwater level in Large Bowl rises because of infiltration and large inflow from the upstream boundary. Once the groundwater level reaches the top elevation of the divide at the saddle location, groundwater flows over the saddle and moves westward down-gradient to the B58 boundary (Fig. 10b). The westward groundwater flow could be critical because it may transport contaminants to downstream areas.

In the B7 subsystem, the groundwater level remains relatively high within the Moraga and Mixed unit. This high groundwater level is the continuation of the groundwater level of the South Orinda subsystem and is maintained locally by the low hydraulic conductivity. For example, the Moraga hydraulic conductivity in this area is 5.10×10^{-8} m s^{-1}, which is one order of magni-

tude lower than that in Small Bowl. The subsystem receives recharge (i) from the South Orinda subsystem, (ii) from infiltration through unpaved areas by rainfall, and (iii) from leaking storm drains located in this subsystem. Groundwater in this subsystem flows into the Large Bowl subsystem as a result of steep hydraulic gradients. In wet, winter seasons, the leakage of the storm drain in the north edge of Building 7 leads to significant flow into the Large Bowl subsystem, corresponding to a seasonal increase in the groundwater level. Figure 11b shows the significant fluctuations in the groundwater level at MW7B-95-25, a representative monitoring well in the B7 subsystem, with a maximum amplitude of 4.57 m (15 feet). The hydrographs measured at 10 monitoring wells in this subsystem are not as smooth as those in the Large Bowl subsystem, indicating that the subsystem responds strongly to short-term episodic rainfall events. This is because the hydraulic conductivity and "effective" porosity in this subsystem are much smaller than elsewhere. Note that the measured hydrograph after April 1997 was affected by the operation of the B7 trench system. In dry, summer seasons, additional water was injected into a well located at the former sump to flush contaminated soil as a remediation measure. As a result, the measured fluctuations in the groundwater level are smaller after the operation of the trench system.

Figure 10 also shows a noticeable amount of groundwater flow going through the Small Bowl subsystem. This system receives water (i) from the upstream Orinda area and (ii) from recharge through the unpaved areas and leaking underground utilities at two locations. Without leakage from the underground utilities, the predicted groundwater level would be much lower than the measured groundwater level. In the upstream portion of this subsystem, the groundwater level fluctuates within the Moraga unit and Mixed units with an amplitude of approximately 3.0 m (Fig. 11c). At the downstream end of the subsystem, however, the groundwater level is in the overlying surficial soils. These have a high effective porosity, leading to relatively small seasonal fluctuations in the groundwater level.

In most of the South Orinda subsystem, groundwater flow is within the Orinda unit, which has a small hydraulic conductivity. However, in the northern area of Building 25, the Orinda unit is more permeable than elsewhere. Measured hydraulic conductivities in this area range from 10^{-4} to 10^{-6} m s^{-1}, with a geometric mean of 1.3×10^{-5} m s^{-1}, while the calibrated value is 1.5×10^{-6} m s^{-1}. As a result of this relatively high hydraulic conductivity, noticeable flow can be seen originating from the upstream boundary. It is this flow that recharges into Small Bowl. Another fraction of this flow moves into South Bowl and proceeds in a southern direction. Local groundwater level elevations can be seen in winter seasons (Fig. 10b), occurring mainly in the unpaved areas where the hydraulic conductivity of underlying units is small.

We now discuss the accuracy of the calibrated model with respect to the observed match between the measured and simulated groundwater level data in Fig. 11. This figure includes the calibration period (1994–1996) during which the measured data have been used for calibrating the model, and the validation period (1996–1998) during which the calibrated model has been applied without previous knowledge of the measured results. Excellent agreement is obtained at Monitoring Well MW53-93-17 in the Large Bowl subsystem regarding the seasonal maximum and minimum groundwater levels, the response time of groundwater level to infiltration events, and the difference between subsequent years with varying rainfall patterns. Similar agreement is obtained at the other monitoring wells in this subsystem, indicating that the flow model can accurately predict groundwater flow in this subsystem. Figure 11b shows good agreement between the predicted and the measured groundwater level at monitoring well MW7B-95-25 in the B7 subsystem. The calibrated flow model reproduces the seasonal fluctuations in the groundwater level measured in the well. However, it should be noted that the recharge through the B7 leaking underground storm drain and the small "effective" porosity calibrated for this subsystem are model features essential to giving good agreement. Figures 11c and 11d show the reasonable agreement at Monitoring Well MW6-92-17 within the Small Bowl subsystem, and at Monitoring Well MW5-93-10 within the South Orinda subsystem.

Another validation method is to compare simulated and measured flow rates at a groundwater collection trench. Figure 12 shows the good match between the predicted flow rate at the B46 boundary group and the measured flow rate at the B46 trench, both in terms of transient patterns and minimum and maximum fluxes. In wet, winter seasons, the highest flow rates in both predicted and measured processes match very well, while the predicted minimum flow rate is larger than the collected one in dry, summer seasons. Possibly, the bottom surface elevation of the Moraga unit in this area is underestimated in the geologic model, so the simulation overestimates flow through this permeable unit in summer months. Accurate description of the hydrogeology in the channel near the B46 boundary is critical for an accurate prediction of the minimum flow rate.

As stated above, the groundwater source to the Old Town system is from (i) recharge by rainfall on unpaved areas, (ii) recharge from the leaking storm drains or underground facilities, and (iii) the inflow from the upstream boundary with higher water table than the downstream boundary segments. To assess the relative significance of these contributions, Table 1 lists the mass balance from the simulation results, in terms of annual average values of recharge, outflow, and mass storage. The most important boundary inflow is from the saturated cross-section area of the Moraga unit on the northeast side of Building 52, although the net areal recharge through unpaved areas and the recharge through leaking underground facilities are also important. The outflow through the boundary segment of B46 accounts for 81% of the total outflow, while that through the B58 boundary segment accounts for 12%. Note that the annual water budget is calculated from 1 July of a year to 30 June of the next year. We can see a large mass storage obtained at the end of the validation period (30 June 1998) because

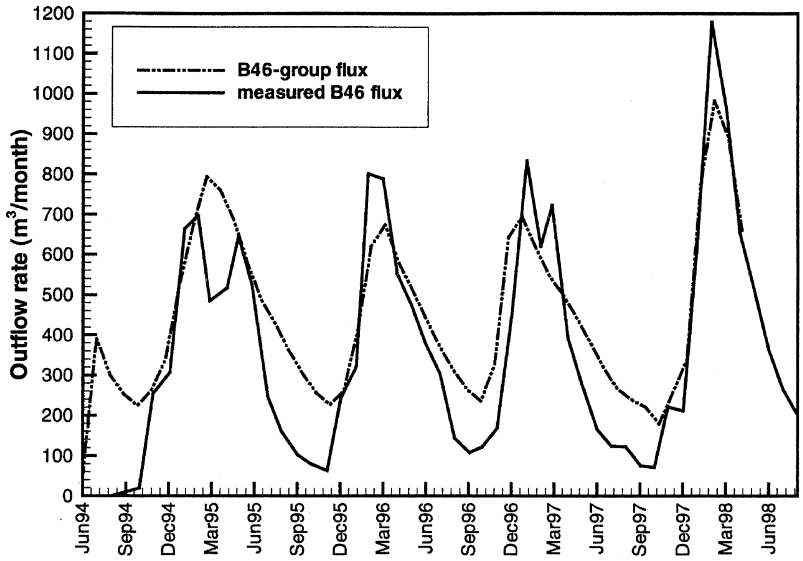

Fig. 12. Comparison of predicted water flow rate at the B46 boundary group and measured flow rate at the B46 trench.

a high water table is still maintained on the boundary (Fig. 11). The mass balance error is small for the system because TOUGH2 is locally and globally mass conservative.

Advective Transport Results

The calibrated flow model is further validated using the measured groundwater contamination plumes. The streamlines of particles originating from contaminant plumes are compared with the extent of the plumes. Simulated steady-state flow fields, representative of the different seasons, are selected to show the development of the plume trends under summer and winter conditions. Figure 13 shows the streamlines of particles originating from selected locations within the plumes using the steady-state flow conditions in August 1997 and March 1998. We focus on the B7 lobe, the main contamination plume, and on the B52 plume, which also migrates toward the B46 boundary.

In August 1997, the particles originating from the upstream portion of the core area of the B7 lobe move to the north, but encounter a region with very small velocity. The particles from the south of the core area move toward the B58 boundary. In March 1998, almost all particles from the core area migrate in the northwest direction toward the B58 boundary. Particles from the low-concentration area south of the core area migrate toward the B58 boundary in both summer and winter seasons, while particles originating from the low-concentration area north of the core area move in the northern direction toward the B46 boundary. Using the August 1997 flow field, no flow occurs through the saddle of the geologic divide, and no particles are found to cross the divide toward the B58 boundary. In March 1998, however, the groundwater level in Large Bowl is elevated by strong winter rainfall events (Fig. 11). As a result, groundwater flows through the saddle toward the B58 boundary, carrying some particles that have originated in the north edge of the core area of the B7 plume.

Table 1. Water budget of the Old Town groundwater system, 1996 through 1998.

	1996–1997	1997–1998
	m³	
Inflow through net areal recharge	1529	2941
Inflow through leaking underground facilities	536	1030
Inflow through the B52 boundary segment	3361	2874
Inflow through the B25 boundary segment	1092	1136
Inflow on other upstream boundary segments	147	149
Outflow through B46 boundary segments	−5400	−5510
Outflow through B58 boundary segments	−844	−796
Outflow through other downstream boundary	−418	−463
Change in mass storage	−43	1570
Mass balance error	46	212

Overall, the pathways of particles originating from the B7 plume lobe are in good agreement with the measured contaminant plumes. The particles originating immediately south of the core plume and all particles from the core area in winter seasons move toward the B58 boundary. This is consistent with the trend of the main B7 plume because the plume is elongated primarily in the northwest direction. Particles originating north of the core plume move northward in summer seasons along the western edge of Large Bowl and the eastern edge of the geologic divide. This is consistent with the elongated plume of low concentrations in the north direction. Note that this part of the plume has smaller concentrations than the core plume. This is because clean groundwater flows into Large Bowl from the upstream boundary, thus diluting the contaminant plume. The other reason is that particles from the north portion of the core area of the B7 lobe move in the north direction only in summer seasons with small travel velocity, resulting in less contaminant mass to the north than that to the northwest direction. More contaminant mass migrates in the northwest direction because of more particles and larger velocity in winter seasons. The consistency between the measured plumes and the particle pathways indicates that the groundwater flow model can reproduce the flow fields reasonably well.

All particles originating at the B52 plume lobe move along with the groundwater toward the B46 boundary

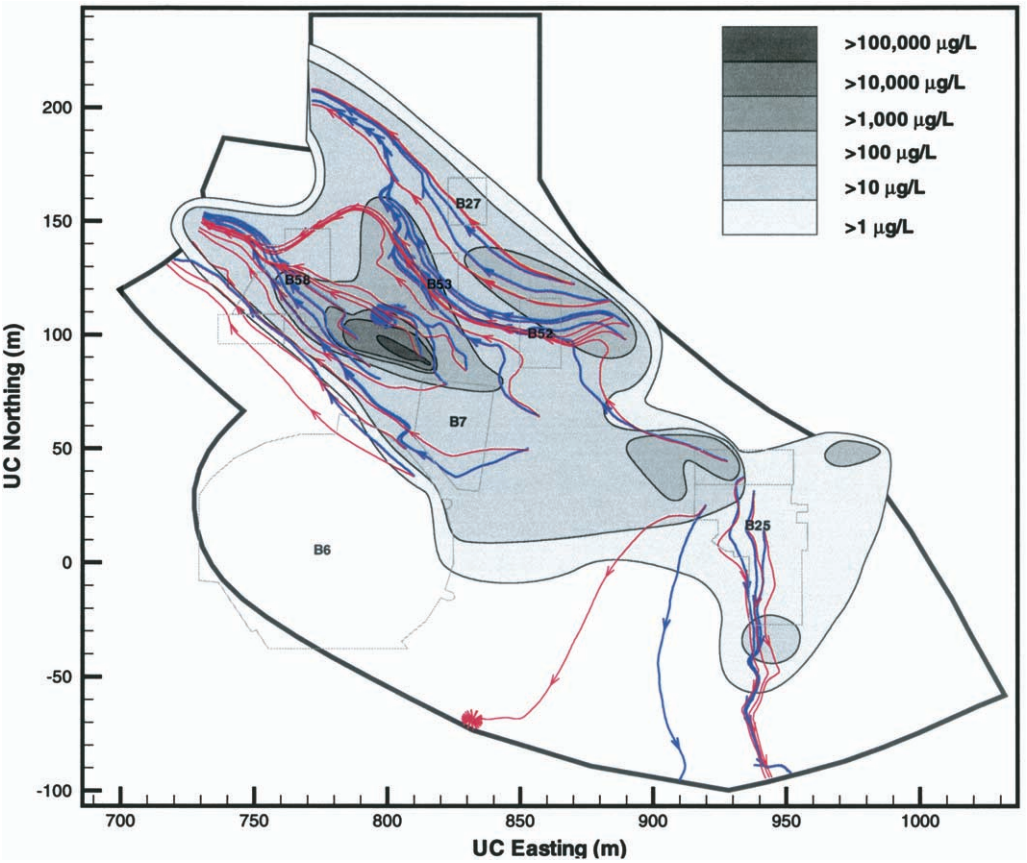

Fig. 13. Trajectories of particles originating from contaminant plumes using steady-state flow in August 1997 (blue lines) and March 1998 (red lines).

in August 1997. In March 1998 (winter seasons), some particles move westward, combine with contaminants originating from the B7 plume lobe, and move further toward the B58 boundary through the saddle of the geologic divide. The measured plume is elongated toward the B46 boundary, similar to the main particle flow direction. Therefore, the pathways of the particles and the elongated plume are in good agreement. In addition, mingling of particles originating from the B52 and B7 plume lobes in winter seasons is also consistent with the formation of a large contaminant plume for the low-concentration contour line.

ASSESSMENT OF HYDRAULIC MEASURES FOR REMEDIATION

The site-scale groundwater flow model is refined to assess the efficiency of existing hydraulic measures in restoring the contaminated site. The refinement is conducted with focus on the main contaminant plume (the B7 lobe), therefore excluding the large area in the south of the site-scale model (Fig. 14). The refined model covers the northern area of the site-scale model, incorporating the B7 plume lobe and the B52 lobe. All perturbations in the groundwater system, such as pumping and injection, are considered in the refined model. The efficiency of two trenches located within the model area (for source control) and two trenches located on the model boundaries (for avoiding contamination of the surrounding environment) is assessed using this refined model. Conditions at the external boundary and initial conditions at 1 June 1996 are based on the simulated groundwater level of the site-scale model. The simulation time is from 1 June 1996 to 30 June 2000.

Perturbations to the global flow fields caused by the operation of two internal trenches are considered in the

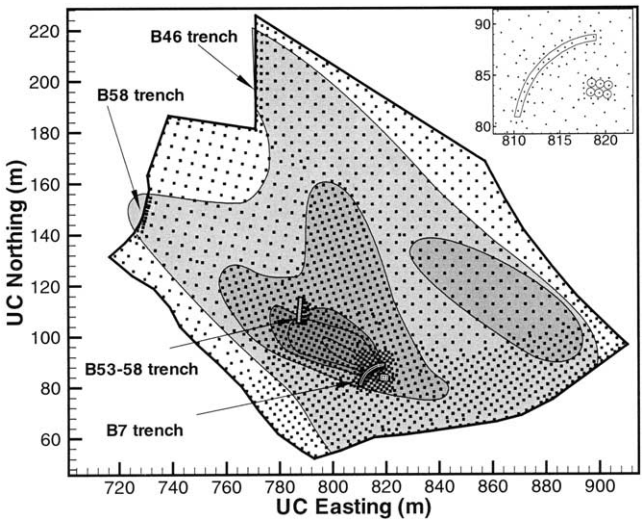

Fig. 14. Boundary and plan view of the three-dimensional mesh for the refined model, with four trenches implemented for restoration. The background is the measured concentration contour with the contour legend shown in Fig. 13. The right upper-corner plot shows a close-up view of the sump and the B7 trench system for controlling the contaminant source.

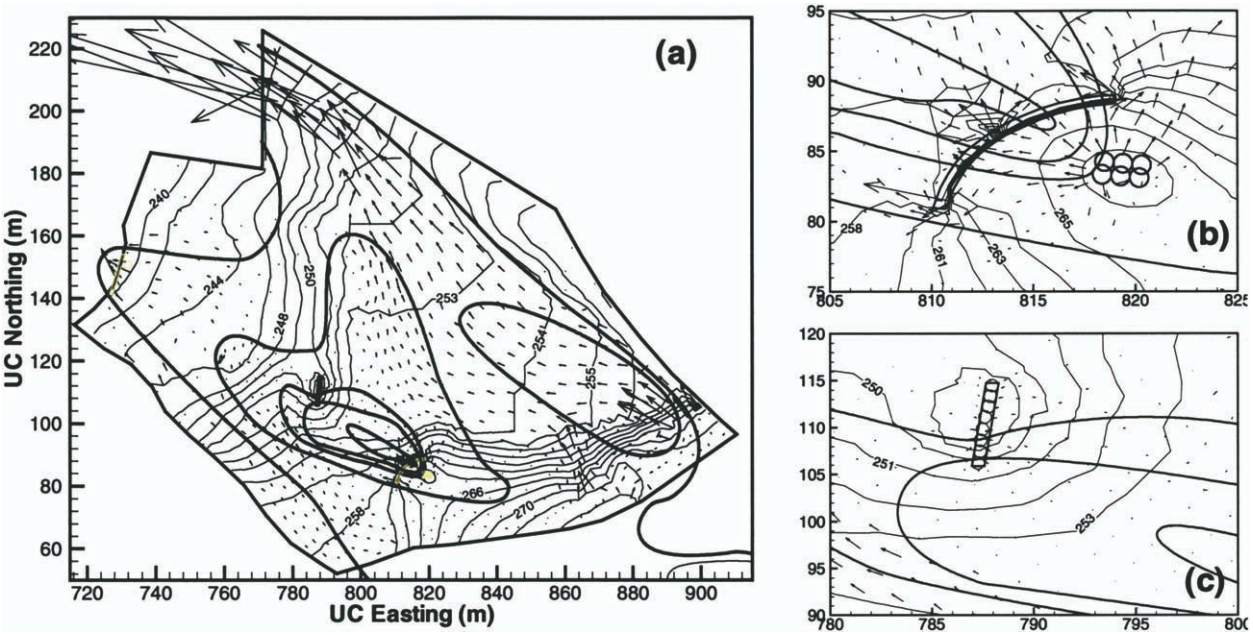

Fig. 15. Contour of the predicted groundwater level (light lines) and flow velocity vector fields on the water table in October 1999 for the refined model in (a) the entire model domain, (b) in the vicinity of the B7 trench, and (c) in the vicinity of the B53-B58 trench. Note that the contaminant plume contour lines are indicated by thick lines (for scales, see Fig. 13).

refined model. Groundwater is pumped at the B7 trench, treated, and continuously reinjected at the upstream sump, which is represented by six vertical columns in the model that are maintained at the measured water table of 266.82 m (Fig. 14). The B7 trench is composed of two trench segments of filled gravel that are separated by a short segment of bedrock, each of which is represented by six vertical columns in the computational mesh. The boundary conditions in the two segments are specified using the measured groundwater level at two extraction wells within the trench. At the B53-58 trench, groundwater is also pumped, treated, and reinjected into the system. This trench is composed of eight gravel-filled columns, and the groundwater level at each column is specified at constant values, varying from 246.89 to 250.48 m.

Figure 15 shows the simulated groundwater level contours and velocity vectors on the water table in October 1999, which represents a dry season. The elevated groundwater level upstream from the B7 trench is caused by the reinjection of treated groundwater at the former sump. Downstream from the B7 trench, the groundwater level decreases as a result of the pumping in the B7 trench. The groundwater from the sump to the trench flows mainly within the permeable Moraga unit, resulting in large recirculation fluxes. The trench is about 17.5 m deep from the groundwater surface, with its bottom in the Orinda unit. Thus, in the vertical direction, the trench controls almost the entire contaminated groundwater flow, because the contamination occurs only in the Moraga and the top portion of the Mixed unit. A mass balance indicates that the trench is capable of capturing about 70% of the groundwater injected at the sump.

The B53-B58 trench was installed in May 1999, based on the observed concentration contour measured at that time. This trench was expected to control the B7 plume at the downstream end of the high concentration portion. It is about 11 m deep from the ground surface, penetrating the Mixed unit (7.5 m thick) and ending in the Orinda unit. The water level imposed at the B53-B58 trench is lower than that in the surrounding area, resulting in convergent groundwater flow toward the trench. However, since the trench is located at the geologic divide and within the Mixed or Orinda unit of low hydraulic conductivity, the amount of groundwater flowing toward the trench is less significant than that in the B7 trench. The simulated flow field and the concentration field recently observed indicate that this trench may not control the contaminant source well because a major fraction of the contaminants migrates along the south of the trench without being captured.

At the B58 trench, the large flow velocities indicate that the trench is effective in preventing contaminated groundwater from leaving the model area and contaminating the surrounding environment. The concentration field suggests that the trench can be used to collect most of the advective flux of contaminants flowing through the B58 boundary. The same conclusion can be drawn for the B46 trench, which collects large amounts of contaminated groundwater for further treatment. However, in light of the differences between summer and wet winter conditions (Fig. 13), there is the possibility during wet seasons that contaminants may migrate through the saddle toward the B58 boundary instead of proceeding toward the B46 trench. Further investigation is needed to evaluate whether these contaminants are being captured in the B58 trench.

CONCLUSIONS

1. In the late 1980s groundwater contamination was detected at the Old Town Area of the Lawrence

Berkeley National Laboratory. Since then, a large amount of data was collected on stratigraphy, hydrogeologic properties, groundwater levels, and contaminant concentrations. Interim corrective measures were initiated to prevent further spreading of contaminants. We describe the development of and simulation results from a three-dimensional transient groundwater flow model designed to (i) improve our basic understanding of the flow and contaminant transport patterns and (ii) to support the decision-making process for remediation measures.

2. A detailed geologic model was developed to describe the complex hydrogeology at the mountainous site, featuring several geologic units with strongly varying thickness and steep slopes. Based on detailed information from several hundred boreholes, a unique geologic setting was identified, with three isolated bowl-shaped rock masses of the Moraga unit embedded in heterogeneous bedrock of much lower permeability (i.e., the Mixed and the Orinda units). Another modeling challenge is the strong seasonal patterns of groundwater flow, mainly affected by significant water recharge from upstream steep hills. In such a setting, the definition of appropriate model domain and boundary conditions is complicated, but essential to model development. In the model, the relevant model boundary passes through a number of groundwater monitoring wells, and the measured transient groundwater levels in these wells were used for boundary conditions.
3. The groundwater model was calibrated using groundwater levels and fluxes collected between 1994 and 1996. The rock zone method was used to deterministically define the spatial variability of rock properties within the same geologic unit, based on the observed clustering characteristics of measured hydraulic conductivities. A composite model was used to account for the internal heterogeneity of the rock, with thin permeable sand layers located within solid rock of low hydraulic conductivity. Transient inverse modeling was conducted to obtain the effective hydraulic conductivity and porosity for each of the 17 defined rock zones. Also calibrated were recharge factors for areal infiltration through rainfall and local infiltration through leaking underground utilities. It was found that local recharge from confirmed leaking storm drains is critical to accurate simulations because it significantly affects the groundwater levels measured in low-permeability areas. Also note that the calibrated effective porosity values are considerably smaller than the actual physical porosity of the rocks. Such small effective porosities demonstrate that only the thin sandstone layers embedded in the bedrock of low hydraulic conductivity are hydraulically important. These small porosities explain the rapid groundwater level changes observed in response to precipitation events.
4. The calibrated groundwater flow model was validated using a blind model prediction conducted for the period between July 1996 and June 1998. The calibrated model produces good matches between the simulated and measured groundwater level in a large number of monitoring wells and also captures the trend observed in the flow rates measured at two groundwater collection trenches. In addition, the simulated advective transport based on particle tracking is in good agreement with the measured extent of contaminant plumes. The validation results indicate that the developed model can accurately predict the complex groundwater flow at the LBNL site.
5. Finally, the calibrated and validated model was refined to focus on the main contaminant plume and on the effects of the perturbations caused by hydraulic measures for remediation. The assessment of hydraulic measures concludes that most of the hydraulic measures are efficient in controlling the contaminant sources and in collecting contaminated groundwater to prevent contamination from entering the surrounding environment. However, one trench may need to be relocated to control the high-concentration area of the main plume. The groundwater flow model provides a valuable tool for improving the decision-making process with respect to the site remediation, and can be used as the basis for further development of a contaminant transport model.

ACKNOWLEDGMENTS

We would like to thank two anonymous reviewers for their insightful and constructive comments and suggestions for improving the paper. We are indebted to Curtis Oldenburg, the Associate Editor, for a careful and thorough reading of the paper. This work is part of the Berkeley Lab's Environmental Restoration Program, supported by the Office of Environmental Management of the U.S. Department of Energy.

REFERENCES

Bandurraga, T.M., and G.S. Bodvarsson. 1999. Calibrating hydrogeologic parameters for the 3-D site-scale unsaturated zone model of Yucca Mountain, Nevada. J. Contam. Hydrol. 38(1–3):25–46.

Bear, J., C.-F. Tsang, and G. de Marsily. 1993. Flow and contaminant transport in fractured rock. Academic Press, San Diego, CA.

Bodvarsson, G.S., W. Boyle, R. Patterson, D. Williams. 1999. Overview of scientific investigations at Yucca Mountain, Nevada, the potential repository for high-level nuclear waste. J. Contam. Hydrol. 38(1–3):3–24.

Bodvarsson, G.S., H.-H. Liu, R. Ahlers, Y.-S. Wu, and E. Sonnenthal. 2001. Parameterization and upscaling in modeling flow and transport at Yucca Mountain. *In* Conceptual models of flow and transport in the fractured vadose zone. National Research Council, National Academy Press, Washington, DC.

Castro, M.C., and P. Goblet. 2003. Calibration of regional groundwater flow model: Working toward a better understanding of site-specific systems. Water Resour. Res. 39(6):1172. doi:10.1029/2002WR001653.

Dagan, G. 1989. Flow and transport in porous formations. Springer-Verlag, Berlin.

de Marsily, G. 1986. Quantitative hydrogeology: Groundwater hydrology for engineers. Academic Press, New York.

Deutsch, C.V., and V.G. Journel. 1998. GSLIB geostatistic software library and user's guide. Oxford University Press, New York.

Finsterle, S. 1999. iTOUGH2 user's guide. Rep. LBNL-40040, UC-400. Lawrence Berkeley Natl. Lab., Berkeley, CA.

Gelhar, L.W. 1993. Stochastic subsurface hydrology. Prentice Hall, Englewood Cliffs, NJ.
Gelhar, L.W., and C.L. Axness. 1983. Three-dimensional stochastic analysis of macrodispersion in aquifers. Water Resour. Res. 19: 161–180.
Isaaks, E.H., and R.M. Srivastava. 1989. Applied geostatistics. Oxford University Press, Oxford, UK.
Javandel, I. 1990. Preliminary environmental investigation at the Lawrence Berkeley Laboratory. Rep. LBNL-29898. Lawrence Berkeley Natl. Lab., Berkeley, CA.
LBNL. 2000. Environmental restoration program RCRA Facility Investigation Report, Module B. Lawrence Berkeley Natl. Lab., Berkeley, CA.
LBNL. 2003. Site environmental report for 2002. Vol. 1. Rep. LBL-27170. Lawrence Berkeley Natl. Lab., Berkeley, CA.
Rubin, Y. 2003. Applied stochastic hydrogeology. Oxford University Press, New York.
Smith, P.A., A. Gautschi, S. Vomvoris, P. Zuidema, and M. Mazurek. 1997. The development of a safety assessment model of the geosphere for a repository sited in the crystalline basement of northern Switzerland. J. Contam. Hydrol. 26:309–324.
Sun, N.-Z. 1994. Inverse problems in groundwater modeling. Kluwer Acad., Norwell, MA.
Tompson, A.F.B., and L.W. Gelhar. 1990. Numerical simulation of solute transport in three-dimensional, randomly heterogeneous porous media. Water Resour. Res. 26:2541–2562.
Tsang, C.F., Y.W. Tsang, and F.V. Hale. 1991. Tracer transport in fractures: Analysis of field data based on a variable aperture channel model. Water Resour. Res. 27:3095–3106.
Zhou, Q., H.-H. Liu, G.S. Bodvarsson, and C.M. Oldenburg. 2003. Flow and transport in unsaturated fractured rock: Effects of multiscale heterogeneity of hydrogeologic properties. J. Contam. Hydrol. 60:1–30.